Decay of isotropic turbulence at low Reynolds number

N. N. Mansour and A. A. Wray

Citation: Physics of Fluids **6**, 808 (1994); doi: 10.1063/1.868319
View online: http://dx.doi.org/10.1063/1.868319
View Table of Contents: http://scitation.aip.org/content/aip/journal/pof2/6/2?ver=pdfcov
Published by the AIP Publishing

Decay of isotropic turbulence at low Reynolds number

N. N. Mansour and A. A. Wray
NASA Ames Research Center, Moffett Field, California 94035

(Received 23 March 1993; accepted 8 June 1993)

Decay of isotropic turbulence is computed using direct numerical simulations. Comparisons with experimental spectra at moderate and low Reynolds numbers ($R_\lambda < 70$) show good agreement. At moderate to high Reynolds numbers ($R_\lambda > 50$), the spectra are found to collapse with Kolmogorov scaling at high wave numbers. However, at low Reynolds numbers ($R_\lambda < 50$) the shape of the spectra at the Kolmogorov length scales is Reynolds number dependent. Direct simulation data from flowfields of decaying isotropic turbulence are used to compute the terms in the equation for the dissipation rate of the turbulent kinetic energy. The development of the skewness and the net destruction of the turbulence dissipation rate in the limit of low Reynolds numbers are presented. The nonlinear terms are found to remain active at surprisingly low Reynolds numbers.

I. INTRODUCTION

Idealizations are often used in turbulence to make the analysis of the problem manageable and to guide model development. The most basic idealization is the case of isotropic decay. A particularly simple limit of isotropic decay is the final period of decay, for which the Navier–Stokes equations become linear. In this state the transfer term can be neglected, and the energy spectrum ($E(\kappa,t)$) follows the linear decay law,[1]

$$E(\kappa,t) = E(\kappa,0)\exp(-2\nu\kappa^2 t). \tag{1}$$

The integral of the above expression over all wave numbers (κ) yields the time evolution of the turbulent kinetic energy in the final period. The above expression indicates that the decay exponent in this period is a function of the shape of the spectrum. In the limit of $t \to \infty$, the slope of the spectrum at the origin dictates the power law decay. Batchelor and Townsend[2] assumed in effect that in the limit $t \to \infty$, the power spectrum will be of the form,

$$E(\kappa,t) \sim \kappa^4 \exp(-2\nu\kappa^2 t)$$

which yields

$$q^2 \sim t^{-5/2}. \tag{2}$$

Saffman[3] showed that if the initial field is generated by random impulsive forces, a spectrum of the form,

$$E(\kappa,t) \sim \kappa^2 \exp(-2\nu\kappa^2 t) \tag{3}$$

will ensue. Such a spectrum will yield

$$q^2 \sim t^{-3/2}. \tag{4}$$

In an effort to measure the power law exponent in the final period, Ling and Huang[4] performed an isotropic decay experiment in water for a range of Taylor microscale Reynolds numbers between 3 and 70. They found that the transfer of energy remained important at low Reynolds numbers and measured a t^{-2} decay law. Bennet and Corrsin[5] carried out a low Reynolds number experiment in air and also found that the transfer terms remained important at their lowest Reynolds number (≈ 4). These experimental setups and the original experiment of Batchelor and Townsend[2] were not able to carry out the measurements to lower Reynolds numbers ($R_\lambda < 3$) because of the difficulties in keeping the flow isotropic at very low Reynolds number.

In one point closure for low-Reynolds-number turbulence, both the exponent of the power law decay and the dependence of the transfer on Reynolds number guide the form of the model used for the equation of the dissipation rate of the turbulence kinetic energy. More data regarding these issues would help model development. Present day computational resources allow for direct numerical simulations (DNS) of simple turbulent flow fields where all the scales of motion are resolved. These DNS are limited to simple geometries and moderate Reynolds numbers. The problem of the final period of decay seems to be an ideal candidate for investigation using DNS. However, it can be shown from the Navier–Stokes equations that, starting with a spectrum of the form $E(\kappa) \sim \kappa^\sigma$ at low wave numbers, the nonlinear terms will lead to a spectrum where $E(\kappa) \sim \kappa^4$ at low wave numbers for $\sigma \geqslant 4$. On the other hand, starting with $\sigma = 2$, the spectrum will be such that $E(\kappa) \sim \kappa^2$ at low wave numbers for all time. Therefore DNS cannot be used to investigate the decay law in the final period since the results clearly depend on the initial conditions. However, DNS can be used to assess the behavior of the nonlinear terms in the limit of vanishing turbulence Reynolds number.

The objective of this study is to compute the decay of isotropic turbulence at low Reynolds numbers using DNS. We will examine the development of the energy spectrum as a function of Reynolds number, and compute the evolution of the velocity-derivative skewness as a function of Reynolds number. We will also investigate the dependence of the budget of the dissipation rate of the turbulent kinetic energy on Reynolds number.

II. THE DECAY OF THE DISSIPATION RATE

The evolution of the energy spectrum in isotropic decay is given by[6]

 1070-6631/94/6(2)/808/7/$6.00

$$E(\kappa,t)_{,t}=T(\kappa,t)-2\nu\kappa^2E(\kappa,t). \tag{5}$$

Integrating the above equation over all wave numbers yields

$$(q^2/2)_{,t}=-2\nu\int_0^\infty \kappa^2E(\kappa,t)d\kappa=-\epsilon \tag{6}$$

where $q^2/2$ is the turbulent kinetic energy, and ϵ is its dissipation rate.

The equation governing the evolution of ϵ in isotropic decay is

$$\epsilon_{,t}=2\nu\overline{\omega_i\omega_ju_{i,j}}-2\nu^2\,\overline{\omega_{i,j}\omega_{i,j}}, \tag{7}$$

where $\omega_i=\epsilon_{ijk}u_{k,j}$ is the vorticity. The first term on the right-hand side of this equation comes from the nonlinear advection terms of the Navier–Stokes equations and represents growth in the dissipation rate due to vortex stretching, while the second term is negative definite and represents the decay of the dissipation rate due to viscous effects.

A. The rate of production of ϵ

Using isotropic forms for the velocity derivative correlations, Eq. (7) can be rewritten[7]

$$\epsilon_{,t}=\frac{7}{30}SR_\lambda\frac{\epsilon^2}{q^2/2}-2\nu^2\,\overline{\omega_{i,j}\omega_{i,j}} \tag{8}$$

where $R_\lambda=q^2/2\sqrt{20/(3\nu\epsilon)}$ is the Taylor microscale Reynolds number, and S is the negative of the velocity-derivative skewness,

$$S=-\frac{\overline{u_{1,1}^3}}{(\overline{u_{1,1}^2})^{3/2}}. \tag{9}$$

From Eq. (8), we see that the production term is directly related to the skewness (whence the interest of one-point closure modelers in the behavior of the skewness), and that the production term increases with Reynolds number.

B. The rate of destruction of ϵ

The increase of the production rate with Reynolds number must be balanced by a similar increase in the destruction rate to keep ϵ bounded in the limit $R_\lambda\to\infty$. This dependence on R_λ can be shown by using the empirically observed invariance of high wave number spectra in Kolmogorov units. The destruction rate may be written in terms of the energy spectrum as

$$2\nu^2\,\overline{\omega_{i,j}\omega_{i,j}}=4\nu^2\int_0^\infty \kappa^4E(\kappa,t)d\kappa. \tag{10}$$

Using the Kolmogorov length scale, $\eta=(\nu^3/\epsilon)^{1/4}$, and velocity scale, $v=(\nu\epsilon)^{1/4}$, to nondimensionalize the energy spectrum and the wave number in Eq.(10), we obtain

$$2\nu^2\,\overline{\omega_{i,j}\omega_{i,j}}=\left(2\sqrt{\frac{3}{5}}\int_0^\infty(\kappa^*)^4E^*d\kappa^*\right)R_\lambda\frac{\epsilon^2}{q^2/2}, \tag{11}$$

where the superscript * denotes nondimensional variables. The contributions to the integral in Eq. (11) are biased toward the high wave number end of the spectrum because of the $(\kappa^*)^4$ weighting in the integrand. At high Reynolds numbers, we expect that the Kolmogorov scaling will result in a collapse of the spectra at high wave numbers (see for example Chapman[8] for a compilation of experimental data from various flows). The collapse of the spectra in Kolmogorov scaling implies that the integral in Eq. (11) is $O(1)$, and therefore the rate of destruction of the dissipation rate grows with R_λ.

An expression for the destruction term was derived by Smith and Reynolds[9] using the model spectrum

$$E(\kappa)=C_\kappa\epsilon^{2/3}\kappa^{-5/3}e^{-\alpha(\kappa\eta)^m},$$

where C_k, α, and m are constants. They used this expression and a closure model for the ϵ-equation to compute the skewness.

C. A closure for the ϵ-equation

Using an order-of-magnitude analysis, Tennekes and Lumley[10] argued that, at high Reynolds numbers, the production term and the destruction term balance each other to $O(R_\lambda)$ leaving a net $O(1)$ term independent of the Reynolds number. For isotropic flows, the net term in the budget of ϵ is a function of ϵ, q^2, and ν and becomes independent of ν at high Reynolds numbers. From dimensional analysis the right-hand side of Eq. (7) can be modeled as

$$\epsilon_{,t}=-C_2(R_\lambda)\frac{\epsilon^2}{q^2/2}, \tag{12}$$

where $C_2(R_\lambda)$ approaches a finite nonzero limit at large R_λ.

If we assume that isotropic turbulence undergoes a power-law decay,

$$q^2\sim t^{-n}, \tag{13}$$

then

$$\epsilon=-(q^2/2)_{,t}\sim nt^{-(n+1)}. \tag{14}$$

Substituting the relations (13) and (14) into Eq. (12) yields a relation between C_2 and the decay exponent,

$$C_2=\frac{n+1}{n}. \tag{15}$$

We shall use DNS of isotropic flows to compute the skewness S and

$$C_2\equiv-\epsilon_{,t}(q^2/2)/\epsilon^2 \tag{16}$$

as a function of Reynolds number.

III. DIRECT NUMERICAL SIMULATIONS

A. Numerical procedure

1. Numerical integration

The Fourier transformed Navier–Stokes equations are written as

$$(e^{\nu\kappa^2t}\hat{u}_i)_{,t}=e^{\nu\kappa^2t}P_{ij}\hat{H}_j, \tag{17}$$

where $\hat{H}_j=-i\kappa_l\widetilde{u_iu_j}$ is the Fourier transform of the nonlinear terms and $P_{ij}=(\delta_{ij}-\kappa_i\kappa_j/\kappa^2)$ is the projection op-

erator required to impose incompressibility. The form allows for exact integration of the viscous terms in a differencing scheme. The numerical procedure used to integrate Eq. (17) is described in detail in Rogallo.[11] In brief, a second-order Runge–Kutta scheme is used to advance in time. The nonlinear terms are computed in real space and are dealiased using a combination of masking and phase shifts. The length scale is set so that the length of the sides of the periodic computational cubic box is 2π, and the velocity scale is taken to be the root mean square (RMS) of the initial (random, isotropic) velocity.

2. Initial conditions

The initial field is generated in Fourier space such that it satisfies continuity and has a prescribed energy spectrum, but otherwise is random and isotropic. This is achieved by setting,[11]

$$\hat{u}_i(\kappa)=\alpha e_i^1+\beta e_i^2, \tag{18}$$

where e_i^1, e_i^2 are mutually orthogonal unit vectors in the plane orthogonal to the wave vector, and α and β are complex coefficients given by

$$\alpha=\left(\frac{E(\kappa,0)}{4\pi\kappa^2}\right)^{1/2}\exp(i\theta_1)\cos(\phi),$$

and

$$\beta=\left(\frac{E(\kappa,0)}{4\pi\kappa^2}\right)^{1/2}\exp(i\theta_2)\sin(\phi),$$

where θ_1, θ_2, and ϕ are uniformly distributed random numbers on the interval $(0,2\pi)$. $E(\kappa,0)$ was taken to be of the form

$$E(\kappa,0)=\frac{q^2}{2A}\,\frac{1}{\kappa_p^{\sigma+1}}\,\kappa^\sigma\exp\left(-\frac{\sigma}{2}\left(\frac{\kappa}{\kappa_p}\right)^2\right), \tag{19}$$

where κ_p is the wave number at which $E(\kappa,0)$ is maximum, σ is a parameter, and $A=\int_0^\infty \kappa^\sigma\exp(-\sigma\kappa^2/2)d\kappa$.

The choice for α and β results in a field in which each mode with a given wave number magnitude has the same (expected) energy level. In addition, the initial field will have statistically zero derivative-skewness and unrealistic (statistically Gaussian) higher velocity moments. A realistic field develops after some evolution time.

We set $q^2=3$ in the expression for the spectrum given by Eq. (19). This leaves the viscosity [ν, or the inverse Reynolds number based on $(1/2\pi)$ the box size and the initial turbulence intensity] as a parameter. In addition, two other parameters characterize the initial spectrum: σ, the exponent in the power-law decay of the spectrum at low wave numbers, and κ_p, the location of the peak of the spectrum, which is a solely numerical parameter used to control the relationship between Reynolds number and Fourier-space sample sizes. A set of simulations was run at various initial Reynolds numbers by varying these three parameters. The simulations are divided into two sets: the first with $\sigma\geqslant 4$ (Table I), and the second with $\sigma=2$ (Table II).

TABLE I. Direct numerical simulations of decaying isotropic turbulence with $\sigma\geqslant 4$.

σ	κ_p	ν	Mesh	Symbol
4	9	0.003	128^3	⊖ ⊖ ⊖
4	30	0.005	128^3	⋊ ⋊ ×
4[a]	30	0.005	128^3	× × ×
6	15	0.002	128^3	+ · · + · · +
6	40	0.003	128^3	◇ ◇ ◇
4	13	0.001	256^3	⊟ ⊟ ⊟
4	25	0.001	256^3	⊟ ⊡ □
4	40	0.003	256^3	⊡ · □ · ⊡

[a]This case is the same as the previous case except that a different random-number seed was used to generate the initial field.

B. Development of the energy spectrum

Adequate resolution of the scales of motion is of primary importance in any direct numerical simulation of turbulent flow. The resolution must be numerically adequate to achieve acceptably low truncation errors and must also yield a sample size adequate for statistically accurate results. In isotropic decay the resolution of the small scales is judged by the shape of the spectrum at high wave numbers. As a rule of thumb we require that the numerical cut-off wave number be at or beyond $\kappa_{\max}\eta\approx 1$, where $\eta=(\nu^3/\epsilon)^{1/4}$ is the Kolmogorov length scale. In general, poor resolution of the small scales results in dynamically significant energy pile-up at high wave numbers. Additionally, since in homogeneous flows the length scale of the large eddies is not bounded by geometrical constraint (walls, etc.), the computational box size should be large enough to accommodate a large sample of the energy-containing eddies. Ideally, at least an order-of-magnitude drop in the energy from the peak to the lowest wave numbers is desirable. The energy of fully developed isotropic turbulence decays in time while the scales of motion grow; the resulting R_λ decreases with time. Therefore a numerically well resolved, fully developed field will remain well resolved as it decays. However, the integral scales will eventually become comparable to the box length, and the results will suffer from a lack of sample of the large scales.

The evolution of the spectrum as predicted by direct numerical simulation using 256^3 points is illustrated in Fig. 1. In this simulation, we use $\sigma=4$ and $k_p=3$ to set the initial spectrum, and $\nu=0.0007$ to set the Reynolds number. This yields an initial random field where the Taylor

TABLE II. Direct numerical simulations of decaying isotropic turbulence with $\sigma=2$.

σ	κ_p	ν	Mesh	Symbol
2	13	0.001	256^3	⊖ ⊖ ⊖
2	18	0.001	256^3	⋊ ⋊ ×
2	25	0.001	256^3	× × ×
2	30	0.001	256^3	+ · · + · · +
2	40	0.001	256^3	◇ ◇ ◇
2	60	0.004	256^3	⊟ ⊟ ⊟
2	25	0.003	256^3	⊟ ⊡ □
2	25	0.002	256^3	⊡ · □ · ⊡

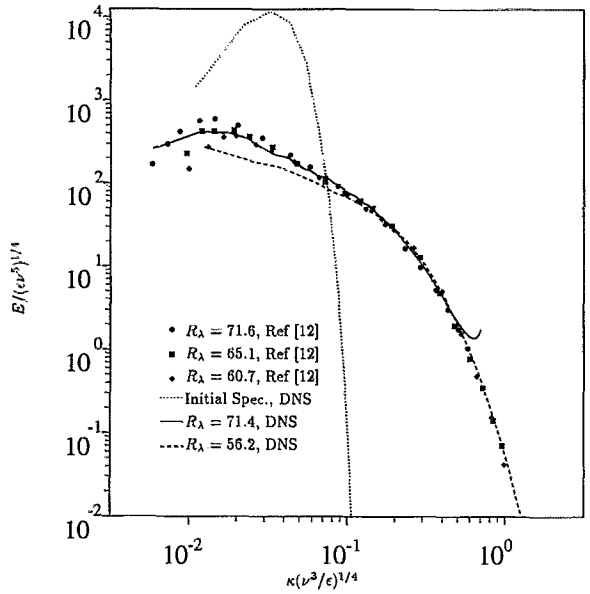

FIG. 1. Spectrum of the energy: comparison with experiment at moderate Reynolds number.

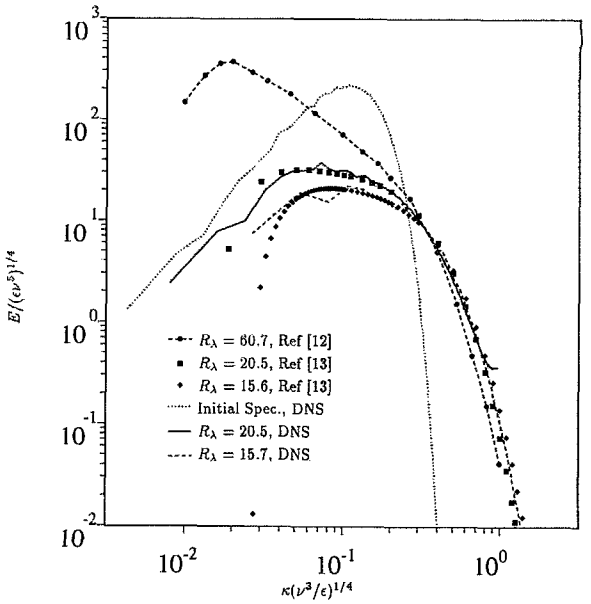

FIG. 2. Spectrum of the energy: comparison with experiment at low Reynolds numbers.

scale Reynolds number $R_\lambda=952$. The initial shape of the spectrum (dotted line in Fig. 1) is unrealistic, but as the flow develops the energy is redistributed to both low and high wave numbers and the Reynolds number decreases. Eventually, a more realistic spectrum evolves, and at $R_\lambda=71.4$ the simulation results match the spectra of Comte-Bellot and Corrsin[12] (hereafter referred to as C-BC) for $\kappa\eta>0.02$. We note that $\kappa_{\max}\eta$ is slightly less than one, indicating that the resolution at high wave numbers is marginal. At low wave numbers the experimental spectra do not collapse, and we do not predict the shape of the experimental spectrum at $R_\lambda=71.6$. In fact our simulation has run out of sample according to the criterion for low wave number drop-off of the energy. This observation was confirmed by examining the distribution of the two-point correlations. We find that the correlation length has become of the same order as our computational box indicating that the box size has become too small. These results indicate that, under our criteria, the maximum R_λ achievable with 256^3 points is that of C-BC. Continuing the simulation results in a flow in which there is an insufficient sample of the large eddies (dashed line in Fig. 1), though the high wave number part of the spectrum still matches the experimental data quite well.

A simulation with 256^3 points was carried out with the initial spectrum shifted toward high wave numbers ($k_p=25$, $\sigma=2$), and the viscosity increased to $\nu=0.001$. In this case, the initial Taylor-scale Reynolds number drops to $R_\lambda=73$. The evolution of the spectrum is shown in Fig. 2, where we compare the predicted spectrum with the recent isotropic decay measurements of Veeravalli[13] at $R_\lambda=20.5$ and 15.6. We have also plotted in Fig. 2 a higher Reynolds number experimental spectrum (C-BC) for reference. We find good agreement between the simulation and Veeravalli's measurements. In particular, the simulation predicts the flattening of the spectra, relative to those found for higher R_λ, in the range $0.1\leqslant\kappa\eta\leqslant0.3$. This flattening implies a low Reynolds number effect on the energy transfer from large to small scales. We also note that the spectra do not follow the same Kolmogorov scaling as those at high Reynolds number.

C. Velocity-derivative skewness

We have pointed out that for isotropic flows the skewness can be directly related to the production of dissipation (or, equivalently, of enstrophy). The skewness is also a measure of the nonlinearity of the Navier–Stokes equations and is a characteristic of turbulent flows. The behavior of the skewness at low Reynolds numbers is of interest since it measures the rate at which the nonlinear energy transfer vanishes as the Reynolds number decreases. Tavoularis, Bennet, and Corrsin[14] (hereafter referred to as TBC) pointed out that the asymptotic behavior of the skewness depends on the behavior of the spectrum at low wave number. Under the assumptions they made, they find that if $E(\kappa)\sim\kappa^4$ as $\kappa\to0$, then

$$S\sim R_\lambda^5 \quad \text{as} \quad t\to\infty,$$

while if $E(\kappa)\sim\kappa^2$ as $\kappa\to0$, then

$$S\sim R_\lambda^6 \quad \text{as} \quad t\to\infty.$$

TBC also measured the skewness for isotropic decay at low Reynolds numbers, and concluded that, while scatter in the data did not permit accurate determination of its asymptotic behavior, it appears that $S\sim R_\lambda^2$ in the range $1<R_\lambda<2$.

We shall define the averages in Eq. (9) to be averages over the computational domain. This implies that our statistical moments are sensitive to the number of moment-contributing eddies that are captured in the computational

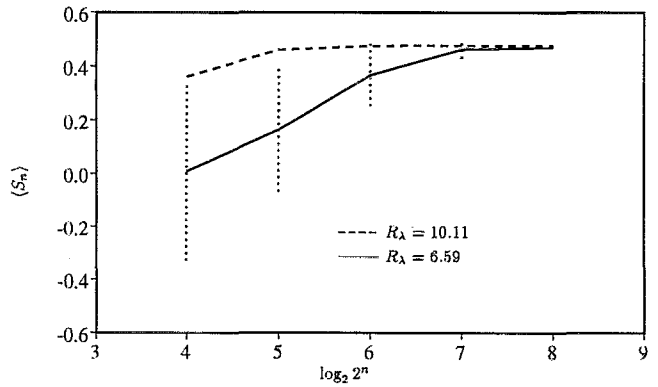

FIG. 3. Skewness as a function of sample size.

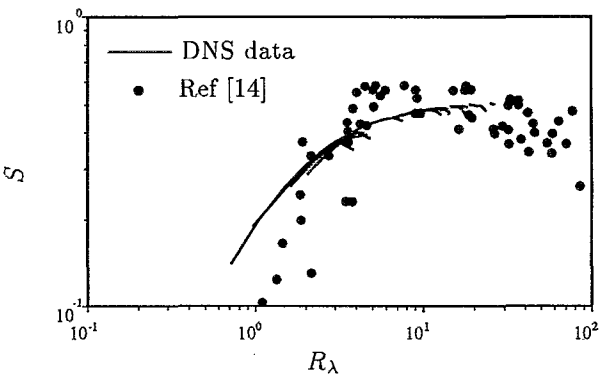

FIG. 5. Velocity-derivative skewness as a function of Reynolds number. The DNS data is the fully developed portion from all the cases.

box. As discussed in the previous section, we heuristically estimate the size of the large-eddy sample from the location of the peak of the spectrum. An estimate for the convergence of our computation of the skewness can be obtained by subdividing our 256^3 box into $(2^{(8-n)})^3$ sub-boxes of size $(2^n)^3$ and computing S_n using Eq. (9) in each sub-box. We expect for $n=0$ (i.e., for a sample with one point) to have the mean over the sub-boxes $\langle S_0 \rangle = 0$ and the standard deviation $\sqrt{\langle S_0^2 - \langle S_0 \rangle^2 \rangle} = 1$. As n increases the standard deviation decreases and $\langle S_n \rangle \to S_8$. The value of $\langle S_n \rangle$ as a function of n is shown in Fig. 3 for the case ($\sigma=2$, $\kappa_p=25$, $\nu=0.003$) at two instant in time. We find that at early times ($R_\lambda=10.11$) when the peak of the spectrum is at high wave numbers, the statistics converge well. As the flow develops, the peak of the spectrum moves to lower wave numbers and the sample of the large eddies decreases. The dotted vertical bars in Fig. 3 show an extent of one standard deviation on either side of the mean at the end of the run ($R_\lambda=6.59$ in this case). The standard deviation at $n=7$ for this case is representative of the order of the error at the end of our runs.

Figure 4 shows the results for the skewness ($S=S_8$) as a function of R_λ from our simulations. The evolution of the skewness starting from initial conditions with $\sigma \geqslant 4$ and $\sigma=2$ is shown in Figs. 4(a) and 4(b) respectively. As expected of a Gaussian random field, the initial skewness is zero. It quickly builds up to a level of the order measured experimentally, but as the flow develops the skewness decreases and then increases to a level that seems to be independent of the initial conditions. The flow field becomes fully developed at this stage, and the high wave number end of the spectra at a given Reynolds number collapse when scaled with Kolmogorov variables. In Fig. 5 we have replotted the data of Fig. 4, removing the results that were thought to belong to the transient stage (but leaving the "tails" to distinguish the curves), and compare the DNS results to the measured skewness data compiled by TBC. The DNS skewnesses are consistent with those measured by TBC. We find that the exponent m in the power-law $S \sim R_\lambda^m$ is not constant in the range $1 \leqslant R_\lambda \leqslant 25$.

D. The decay of the dissipation rate

We have shown in Eq. (15) that if the turbulence undergoes a power law decay, the exponent can be measured by computing $C_2 \equiv -\epsilon_{,t}(q^2/2)/\epsilon^2$. The exponent n of the power law decay is known in the two limits, $R_\lambda \to 0$ and $R_\lambda \to \infty$. In the limit $R_\lambda \to 0$ we expect for $\sigma=4$ [see Eq. (2)],

$$C_2 = 1.4, \tag{20}$$

and for $\sigma=2$ [see Eq. (4)],

$$C_2 = 1.67. \tag{21}$$

Similarly for $R_\lambda \to \infty$, it can be shown rigorously[3] that $n=6/5$ for $\sigma=2$, which yields

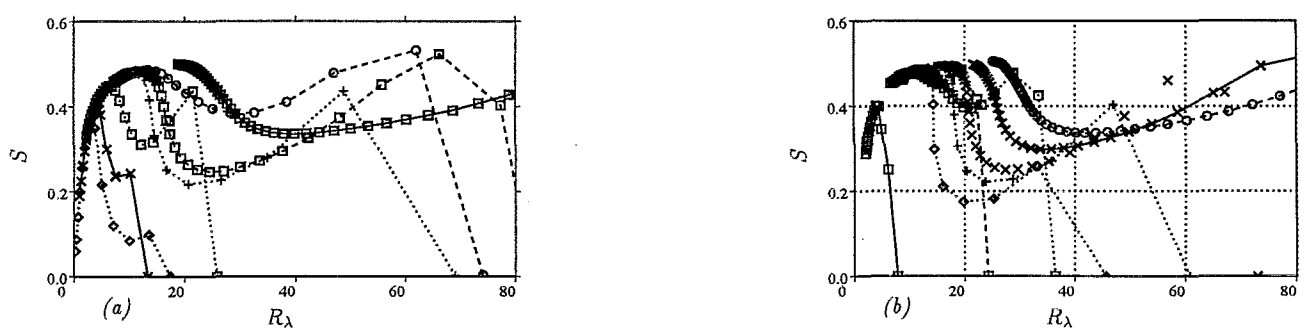

FIG. 4. Velocity-derivative skewness as a function of Reynolds number. (a) $\sigma \geqslant 4$ (for symbols see Table I). (b) $\sigma=2$ (for symbols see Table II).

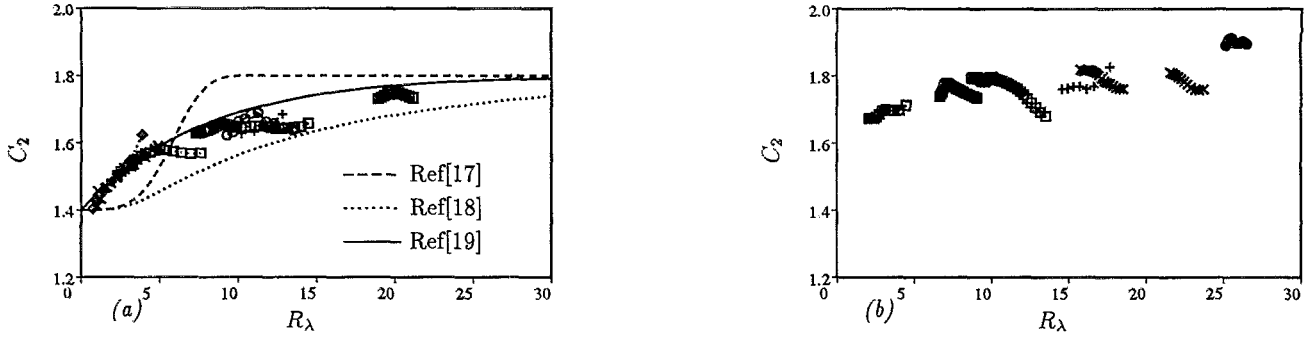

FIG. 6. Development of C_2 as a function of Reynolds number. (a) $\sigma \geq 4$ (for symbols see Table I); (b) $\sigma=2$ (for symbols see Table II).

$$C_2=1.83. \tag{22}$$

This result has been obtained in a simulation by Chasnov.[15] An approximate result, first due to Kolmogorov,[16] is $n \cong 10/7$ for $\sigma=4$, which yields

$$C_2 \cong 1.7. \tag{23}$$

The variation of C_2 with Reynolds number (Fig. 6) is of interest in low-Reynolds-number modeling, and it is reasonable to expect that it varies monotonically with R_λ between the two limits.

C_2 depends on both the large scales (through q^2) and the small scales, and we find from our simulations that it is a sensitive measure of our ability to capture the large scales. The criterion (based on the skewness collapse) that was used to determine when the flow is fully developed seems also to hold for C_2, although the collapse of C_2 is not as good as that of the skewness, probably because it is difficult in a direct simulation to obtain a fully developed field with both well resolved small scales and adequately sampled large scales. The scatter in C_2 for a given Reynolds number is similar to the scatter observed when initial conditions are generated with different seeds for the random numbers, suggesting that these variations are due to the limited size of the statistical sample. Note that the skewness (at fixed R_λ) is independent of the initial conditions, but C_2, which measures the difference between the production rate and destruction rate of ϵ, is somewhat sensitive to the initial conditions. We include in Fig. 6(a) the models for C_2 of Hanjalić and Launder,[17] Lumley[18] and a curve fit to the data suggested by Coleman and Mansour.[19] Note that both Hanjalić and Launder,[17] and Lumley[18] assumed that $dC_2/dR_\lambda=0$ at $R_\lambda=0$, while Coleman and Mansour[19] relaxed this requirement and allowed the slope of C_2 to be nonzero at $R_\lambda=0$.

IV. CONCLUSIONS

We have considered the simplest turbulent flow, isotropic decay, and have shown that with 256^3 points direct numerical simulations are limited to Reynolds numbers not exceeding those found in the experiment of Comte-Bellot and Corrsin.[12] We have shown that there is a low-Reynolds-number effect on the Kolmogorov scales. At Reynolds numbers above $R_\lambda \approx 50$ the shape of the Kolmogorov-scaled spectrum becomes Reynolds number independent at high wave numbers.

The flow fields from these simulations have been used to document the development of the skewness as a function of Reynolds number. The skewness, which depends on moderate to small scales, is independent of the shape of the spectrum at low wave numbers but strongly depends on Reynolds number for $R_\lambda < 5$. We find that the net destruction rate of the dissipation rate is influenced by the shape of the spectrum at low wave numbers. In general, such information is difficult to include in one point closure models.

ACKNOWLEDGMENTS

The authors would like to acknowledge many useful discussions with Drs. R. S. Rogallo, J. R. Chasnov, G. N. Coleman, and R. D. Moser at NASA Ames Research Center. The computational resources of the Numerical Aerodynamic Simulator (NAS) at NASA Ames Research Center are gratefully acknowledged. All direct numerical simulations were performed using the NAS 128 processor iPSC/860 Gamma.

[1] J. O. Hinze, *Turbulence* (McGraw-Hill, New York, 1975).
[2] G. K. Batchelor and A. A. Townsend, "Decay of turbulence in the final period," Proc. R. Soc. London Ser. A **194**, 527 (1948).
[3] P. G. Saffman, "The large-scale structure of homogeneous turbulence," J. Fluid Mech. **27**, 581 (1967).
[4] S. C. Ling and T. T. Huang, "Decay of weak turbulence," Phys. Fluids **13**, 2912 (1970).
[5] J. C. Bennet and S. Corrsin, "Small Reynolds number nearly isotropic turbulence in a straight duct and a contraction," Phys. Fluids **21**, 2129 (1978).
[6] A. S. Monin and A. M. Yaglom, *Statistical Fluid Mechanics,* edited by J. L. Lumley (MIT Press, Cambridge, Massachusetts, 1975), Vol. 2.
[7] W. C. Reynolds, "Physical and analytical foundations, concepts, and new directions in turbulence modeling and simulation," in *Turbulence Models and Their Application,* edited by B. E. Launder, W. C. Reynolds, W. Rodi, J. Mathieu, and D. Jeandel (Eyrolles, Paris, 1984), Vol. 2.
[8] D. R. Chapman, "Computational aerodynamics development and outlook," AIAA J. **17**, 1293 (1979).
[9] L. M. Smith and W. C. Reynolds, "The dissipation-range spectrum and the velocity-derivative skewness in turbulent flows," Phys. Fluids A **3**, 992 (1991).
[10] H. Tennekes and J. L. Lumley, *A First Course in Turbulence* (MIT Press, Cambridge, Massachusetts, 1972).
[11] R. S. Rogallo, "Numerical experiments in homogeneous turbulence," NASA Tech. Memo. TM 81315 (1981).

[12]G. Comte-Bellot and S. Corrsin, "Simple Eulerian time correlation of full and narrow band velocity signals in isotropic turbulence," J. Fluid Mech. **48**, 273 (1971).
[13]S. V. Veeravalli, "An experimental study of the effects of rapid rotation on turbulence," in *Annual Research Briefs—1990* (Center for Turbulence Research, Stanford University, Stanford, CA, 1991), p. 203.
[14]S. Tavoularis, J. C. Bennett, and S. Corrsin, "Velocity-derivative skewness in small Reynolds number, nearly isotropic turbulence," J. Fluid Mech. **88**, 63 (1978).
[15]J. R. Chasnov, "Similarity states of passive scalar transport in isotropic turbulence," Phys. Fluids A **6**, 1036 (1993).
[16]A. N. Kolmogorov, "Decay of isotropic turbulence in incompressible viscous fluids," Dokl. Akad. Nauk SSSR **31**, 538 (1941).
[17]K. Hanjalić and B. E. Launder, "Contribution towards a Reynolds-stress closure for low-Reynolds-number turbulence," J. Fluid Mech. **74**, 593 (1976).
[18]J. L. Lumley, "Computational modeling of turbulent flows," Adv. Appl. Mech. **18**, 123 (1978).
[19]G. N. Coleman and N. N. Mansour, "Simulation and modeling of homogeneous compressible turbulence under isotropic mean compression," *Turbulent Shear Flows 8*, edited by F. Durst, B. E. Launder, F. W. Schmidt, and J. H. Whitelaw (Springer-Verlag, Heidelberg, 1993).